REPORT SD-TR-89-41

4

Photodissociation of XeF_2 at 193 nm

J. F. BOTT, R. F. HEIDNER, J. S. HOLLOWAY, and J. B. KOFFEND
Aerophysics Laboratory
Laboratory Operations
The Aerospace Corporation
El Segundo, CA 90245

30 June 1989

Prepared for

WEAPONS LABORATORY
Kirtland Air Force Base, NM 87117

SPACE SYSTEMS DIVISION
AIR FORCE SYSTEMS COMMAND
Los Angeles Air Force Base
P.O. Box 92960
Los Angeles, CA 90009-2960

This report was submitted by The Aerospace Corporation, El Segundo, CA 90245, under Contract No. F04701-88-C-0089 with the Space Systems Division, P.O. Box 92960, Los Angeles, CA 90009-2960. It was reviewed and approved for The Aerospace Corporation by W. P. Thompson, Director, Aerophysics Laboratory. Lt Scott W. Levinson, SSD/CNID, was the project officer for the Mission-Oriented Investigation and Experimentation (MOIE) program.

This report has been reviewed by the Public Affairs Office (PAS) and is releasable to the National Technical Information Service (NTIS). At NTIS, it will be available to the general public, including foreign nationals.

This technical report has been reviewed and is approved for publication. Publication of this report does not constitute Air Force approval of the report's findings or conclusions. It is published only for the exchange and stimulation of ideas.

SCOTT W. LEVINSON, LT, USAF
MOIE Project Officer
SSD/CNID

JAMES A. BERES, LT COL, USAF
MOIE Program Manager
Director, AFSTC/WCO OL-AB

REPORT DOCUMENTATION PAGE

1a REPORT SECURITY CLASSIFICATION Unclassified	1b RESTRICTIVE MARKINGS
2a SECURITY CLASSIFICATION AUTHORITY	3 DISTRIBUTION / AVAILABILITY OF REPORT Approved for public release; distribution unlimited.
2b DECLASSIFICATION DOWNGRADING SCHEDULE	
4 PERFORMING ORGANIZATION REPORT NUMBER(S) TR-0089(4930-04)-1	5 MONITORING ORGANIZATION REPORT NUMBER(S) SD-TR-89-41
6a NAME OF PERFORMING ORGANIZATION Laboratory Operations The Aerospace Corporation 6b OFFICE SYMBOL (If applicable)	7a NAME OF MONITORING ORGANIZATION Space Systems Division
6c ADDRESS (City, State, and ZIP Code) El Segundo, CA 90245	7b ADDRESS (City, State, and ZIP Code) Los Angeles Air Force Base Los Angeles, CA 90009-2960
8a NAME OF FUNDING / SPONSORING ORGANIZATION Weapons Laboratory 8b OFFICE SYMBOL (If applicable)	9 PROCUREMENT INSTRUMENT IDENTIFICATION NUMBER F04701-88-C-0089
8c ADDRESS (City, State, and ZIP Code) Kirtland Air Force Base, NM 87117	10 SOURCE OF FUNDING NUMBERS PROGRAM ELEMENT NO. / PROJECT NO. / TASK NO / WORK UNIT ACCESSION NO.

11 TITLE (Include Security Classification)
Photodissociation of XeF_2 at 193 nm

12 PERSONAL AUTHOR(S)
Bott, Jerry F.; Heidner, Raymond F.; Holloway, John S.; and Koffend, John B.

13a TYPE OF REPORT	13b TIME COVERED FROM _____ TO _____	14 DATE OF REPORT (Year, Month, Day)	15 PAGE COUNT
		1989 June 30	24

16 SUPPLEMENTARY NOTATION

17 COSATI CODES		
FIELD	GROUP	SUB-GROUP

18 SUBJECT TERMS (Continue on reverse if necessary and identify by block number)
Photodissociation
XeF_2
XeF or xenon fluoride
UV absorption
Excimer lasers
Photolysis

19 ABSTRACT (Continue on reverse if necessary and identify by block number)

The absorption coefficient of XeF_2 has been measured at 193, 206, and 253 nm. The measurements have been compared with those of Black et al. and Jortner et al. The present measurements of XeF_2 absorption at 193 and 253 nm appear to resolve the discrepancy in those absorption measurements. Adjusting the data of the two previous investigations to match our values at these two wavelengths brings the two sets of measured absorption coefficients into agreement in the overlapping wavelength interval, 203 to 210 nm. We determined experimentally that one molecule of XeF_2 is dissociated for each photon absorbed at 193 nm.

20 DISTRIBUTION / AVAILABILITY OF ABSTRACT	21 ABSTRACT SECURITY CLASSIFICATION
☐ UNCLASSIFIED/UNLIMITED ☒ SAME AS RPT ☐ DTIC USERS	Unclassified
22a NAME OF RESPONSIBLE INDIVIDUAL	22b TELEPHONE (Include Area Code) / 22c OFFICE SYMBOL

CONTENTS

FIGURES

I. INTRODUCTION

Interest in the spectroscopy of xenon difluoride (XeF_2) has been stimulated by the xenon fluoride (XeF) laser, which operates on the B-X transitions at 351 and 353 nm and the C-A transitions at 483 nm. The vacuum ultraviolet (VUV) photolysis of XeF_2 can be used either to obtain laser action on these transitions or to produce the several electronic states of XeF for kinetic studies. The XeF_2 photodissociation laser has been pumped by UV sources, such as discharges initiated by exploding wires,[1,2] UV radiation emitted by Xe_2 excited by an electron beam,[3,4] and sliding surface discharges.[5-7]

Modeling the performance of the XeF laser, whether the laser is E-beam pumped, electric-discharge pumped, or photolysis pumped, requires rate coefficients for the kinetic processes that produce and remove the vibronic levels of the upper electronic state (the $B^2\Sigma^+$ state and the coupled $C^2\pi^+$ state) and the lower state ($X^2\Sigma^+$,v"). The UV photolysis of XeF_2 is a convenient method of producing both the B state and the X state of XeF for kinetics studies of the required rate coefficients. B-state kinetic studies have been reported by Eden and Waynant,[8,9] Brashears et al.,[10,11] Black et al.,[12] and Helm et al.[13]

The photolysis of XeF_2 with a 15-nsec ArF excimer laser pulse at 193 nm can produce electronically excited XeF(B), which decays with a 14-nsec lifetime[8] to the ground electronic state, XeF(X,v). It can also produce XeF(X,v) directly. Photolysis of XeF_2 was used by both Fulghum et al.[14,15] and Bott et al.[16] in studies of the dissociation and vibrational relaxation of the ground electronic state of XeF. In designing such experiments, it is helpful to know both the absorption coefficient of XeF_2 and the quantum yield of the products.

Black et al.[12] measured the absorption coefficient of XeF_2 between 145 and 210 nm and the quantum yield between 145 and 175 nm. Jortner et al.[17] measured the absorption coefficient from 203 to 280 nm. The present study was directed to resolving the discrepancy in the previous two sets of

measurements in the overlapping region of 203 to 210 nm and to determining the absorption coefficient at 193 nm, the wavelength of the ArF laser used in several kinetic studies. The quantum yield for the dissociation XeF_2 was also measured at 193 nm.

II. EXPERIMENTAL MEASUREMENTS

A. ABSORPTION BY XeF_2

A schematic of the experimental apparatus is shown in Fig. 1. The main elements include a flow cell and gas handling system, a Lambda Physik excimer laser (ArF), a Bausch and Lomb 1/4-m monochromator, a photomultiplier, a Stanford Research Systems model SR 250 boxcar averager, and a DEC 11/23 computer for data acquisition and storage. The experimental apparatus are also described in Ref. 16.

Room temperature measurements were made in a 5-cm-diam flowtube of stainless steel and two sections of anodized aluminum. The flowtube is more accurately described as an absorption cell through which gas flows slowly to replenish the photolyzed XeF_2. Flow velocities of 2.5 to 5 cm/sec are controlled by a throttle valve just downstream of the flowtube and an upstream needle valve. The stainless steel was coated with Teflon to reduce the loss of XeF_2 to the walls. Suprasil windows mounted in aluminum and brass window holders define the length of the cell to be 75 cm. A stainless steel mixing vessel holds XeF_2 crystals at their vapor pressure, which is about 4.4 Torr at 298 K.[18] Baratron gauges measure the pressures in the flowtube and in the XeF_2 reservoir, and thermocouples measure the temperature of the absorption cell.

A second flowtube designed for studies at elevated temperatures is a straight copper tube with window flanges on the ends and inlet and outlet ports for the gas flow. Thermocouples are located at the two ends and in the middle of the flowtube. The copper tube is wrapped with heating tape and insulation to permit elevated-temperature studies. The distance between the windows is 59.7 cm, although extensions to the tube permit heating outside the windows to ensure a uniform temperature in the flowtube.

The Lambda Physik excimer laser produces 15-nsec pulses with energies of about 100 mJ when lasing on ArF at 193 nm. However, atmospheric

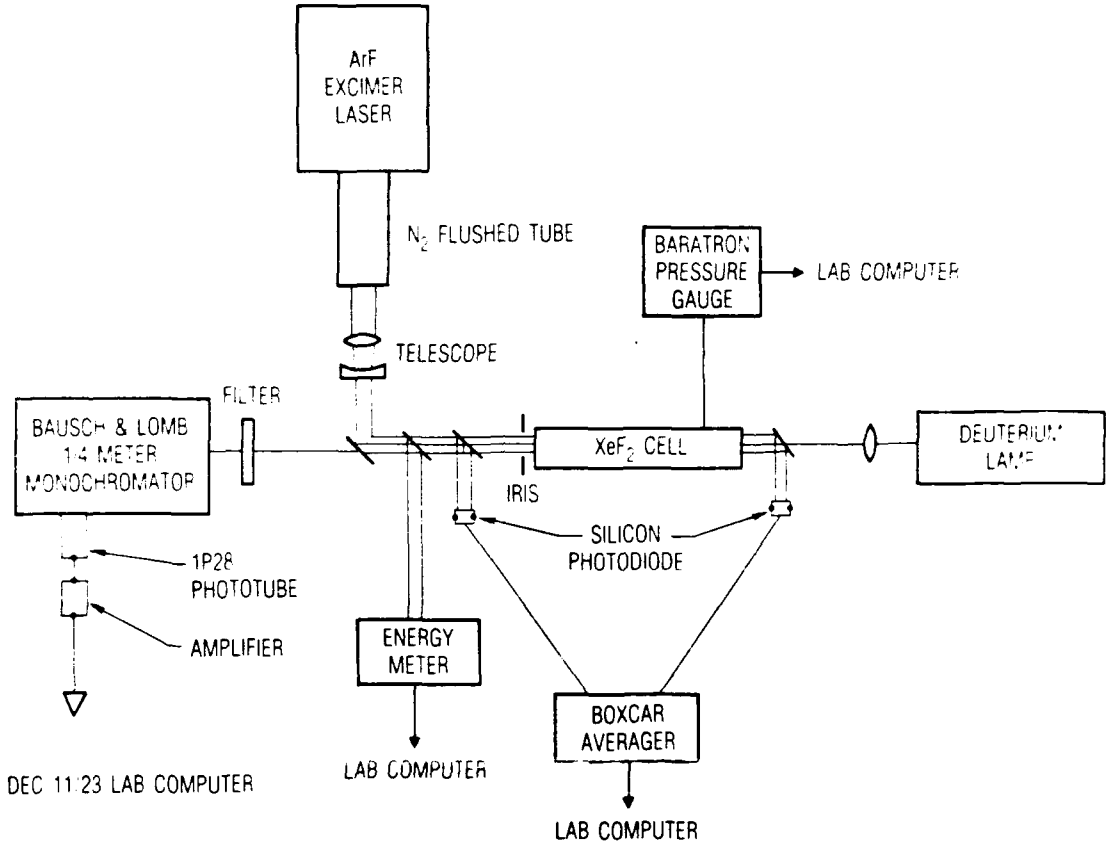

Fig. 1. Schematic of measurement apparatus.

absorption and losses in the optical train attenuate the energy by about a factor of 2, even though the path is partially flushed with nitrogen. The beam is compressed by a factor of 2 with a telescope and turned 90° with a front-surface dielectric mirror. A 10-mm-diam aperture cuts off the edges of the 6- × 12-mm beam. An energy per pulse of about 40 mJ is delivered to the window of the flowtube for photolyzing XeF_2.

Experiments were performed to determine the spectral absorption coefficients of XeF_2 at 193 nm, the wavelength of the ArF laser, and at 253 nm. The ArF laser beam was apertured to 1 mm diam, attenuated a factor of 300 by neutral-density filters, and monitored with silicon photodiodes before and after passing through the absorption cell. Also, the telescope was removed from the optical train. Beam splitters reflected only a small fraction of the beam to the photodiodes to avoid saturating the photodiode signals. The photodiode signals were sent to separate channels of a Stanford Research Systems model SR 250 boxcar averager, whose outputs were recorded with the DEC 11/23 computer. The absorption in the cell could be calculated from changes in the ratio of the attenuated signal to the reference signal.

A collimated beam from a deuterium lamp was passed in the opposite direction, filtered with a Hg line UV interference filter, and monitored with an RCA 1P28 photomultiplier. The photomultiplier signal was amplified and recorded with the computer. The absorption at 253 nm could be recorded simultaneously with the absorption at 193 nm to improve the accuracy of the absorption coefficients relative to each other. Measurements were recorded for XeF_2 pressures between 0.143 and 1.24 Torr; the data are shown in Fig. 2. From these data and a cell length of 75 cm we calculated an absorption coefficient at 193 nm of 0.0262 $(Torr\text{-}cm)^{-1}$ and an absorption cross section of 7.9×10^{-19} cm^2. We obtained a value of 8.0×10^{-20} cm^2 for the absorption cross section at 253 nm.

We measured the absorption coefficient of XeF_2 at 206 nm in a separate experiment in the 59.7-cm-long copper flowtube. The wavelength of 206 nm lies in the 203- to 210-nm spectral range for which both Black et al.[12] and

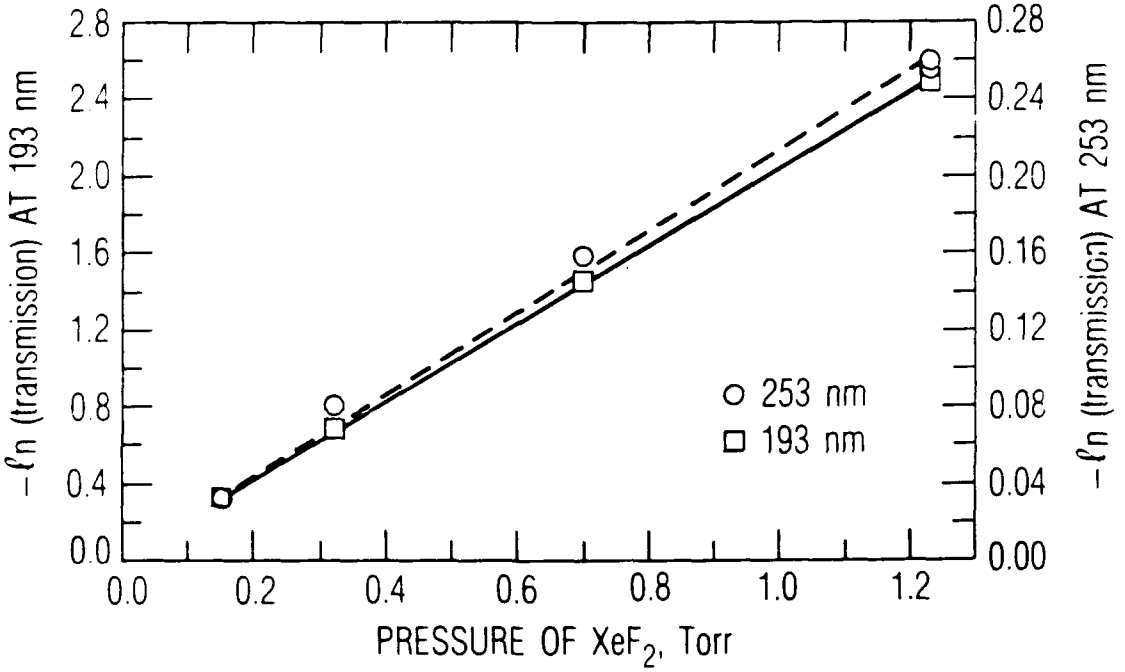

Fig. 2. Plot of XeF_2 absorption [-ℓn(transmission)] versus XeF_2 pressure.

Jortner et al.[17] reported absorption coefficients. The emission from a deuterium lamp was filtered with a 206-nm interference filter and passed through the flowtube to a Bausch and Lomb 1/4-m monochromator and photomultiplier. For this measurement, a chopper was placed in front of the deuterium lamp, and the photomultiplier signal was amplified with a PAR lock-in amplifier. With the flowtube initially evacuated and the XeF_2 reservoir pumped down to its vapor pressure, a low-pressure flow through the flowtube was established. Both the pressure in the flowtube and the photomultiplier signal were recorded by the computer with a 12-bit A-to-D converter. Once the throttle valve was shut the pressure rose to 1.4 Torr in about 1 min. Figure 3 shows the natural logarithm of the transmission plotted versus the pressure, reduced to XeF_2 number density for the temperature of 21°C. From the slope of the data and the 59.7-cm length of the cell, we calculated an absorption coefficient of 2.56×10^{-19} cm^2. These measurements were repeated with the flowtube heated to 81°C, and a somewhat larger value, 2.96×10^{-19} cm^2, was obtained from the data of Fig. 4.

When XeF_2 was isolated in the copper flowtube for 8 min, the absorption decreased 5% or less. This extrapolates to an exponential decay time of 160 min for the XeF_2 density. In contrast, the XeF_2 had a lifetime of about 12 to 15 min in the Teflon-coated stainless steel and aluminum flowtube.

The absorption coefficient and the quantum yield of the photolysis products are of importance to the design of an experiment based on the photolysis of XeF_2. We measured the quantum yield of dissociation products per absorbed photon in the following way. The copper flowtube was filled with XeF_2 to a pressure of 1.34 Torr and isolated with the valves. The ArF laser was used to photolyze the XeF_2, and the pressure in the flowtube was monitored with the Baratron gauge. The energy of the photolysis pulses was monitored with a Laser Precision energy meter; it was calibrated <u>in situ</u> and recorded a measured fraction of the total pulse energy at the entrance to the cell. The energy per pulse is plotted versus time in Fig. 5 for two sequences. Note the break in the laser power at 700 sec and its slow

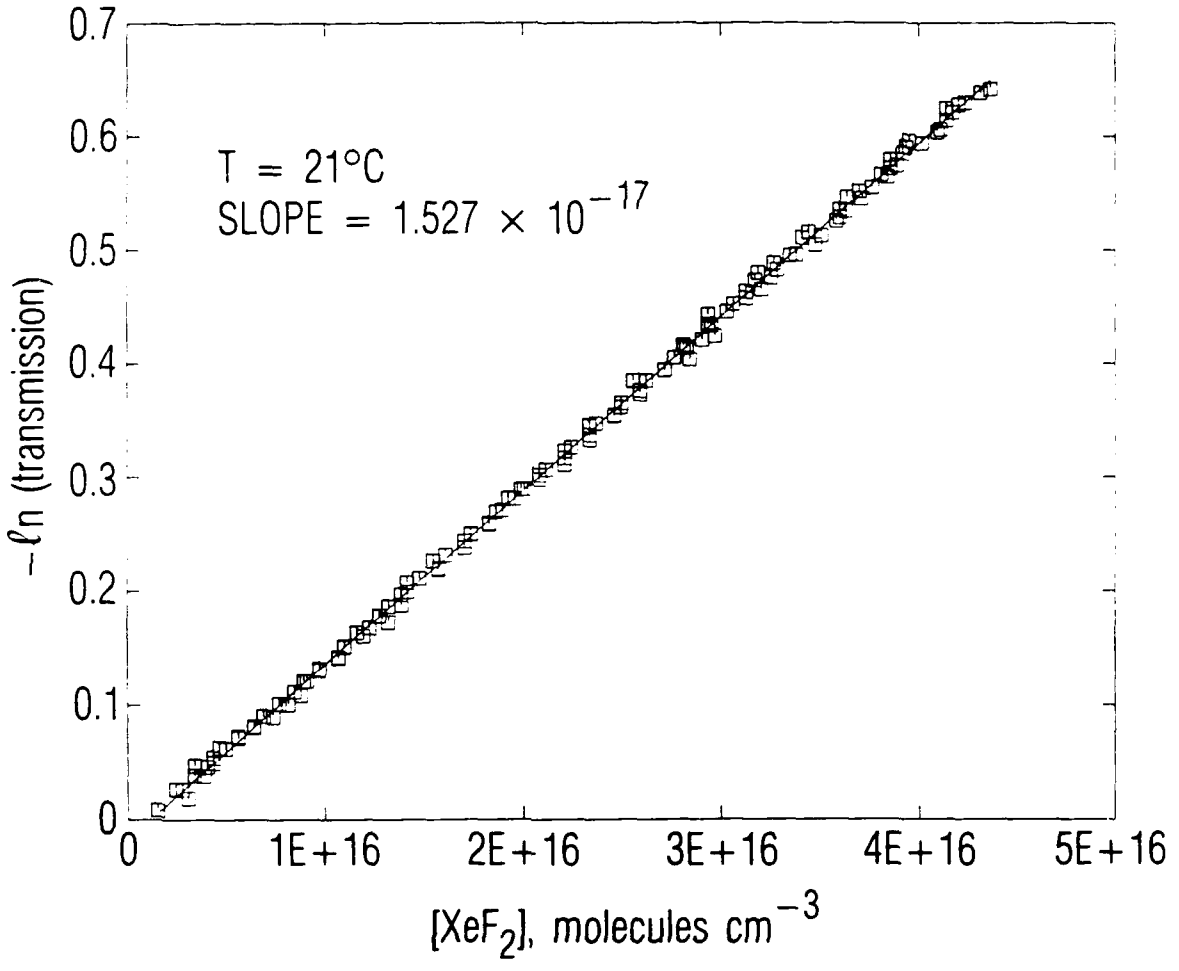

Fig. 3. Plot of XeF_2 absorption [-ℓn(transmission)] at 206 nm versus XeF_2 density.

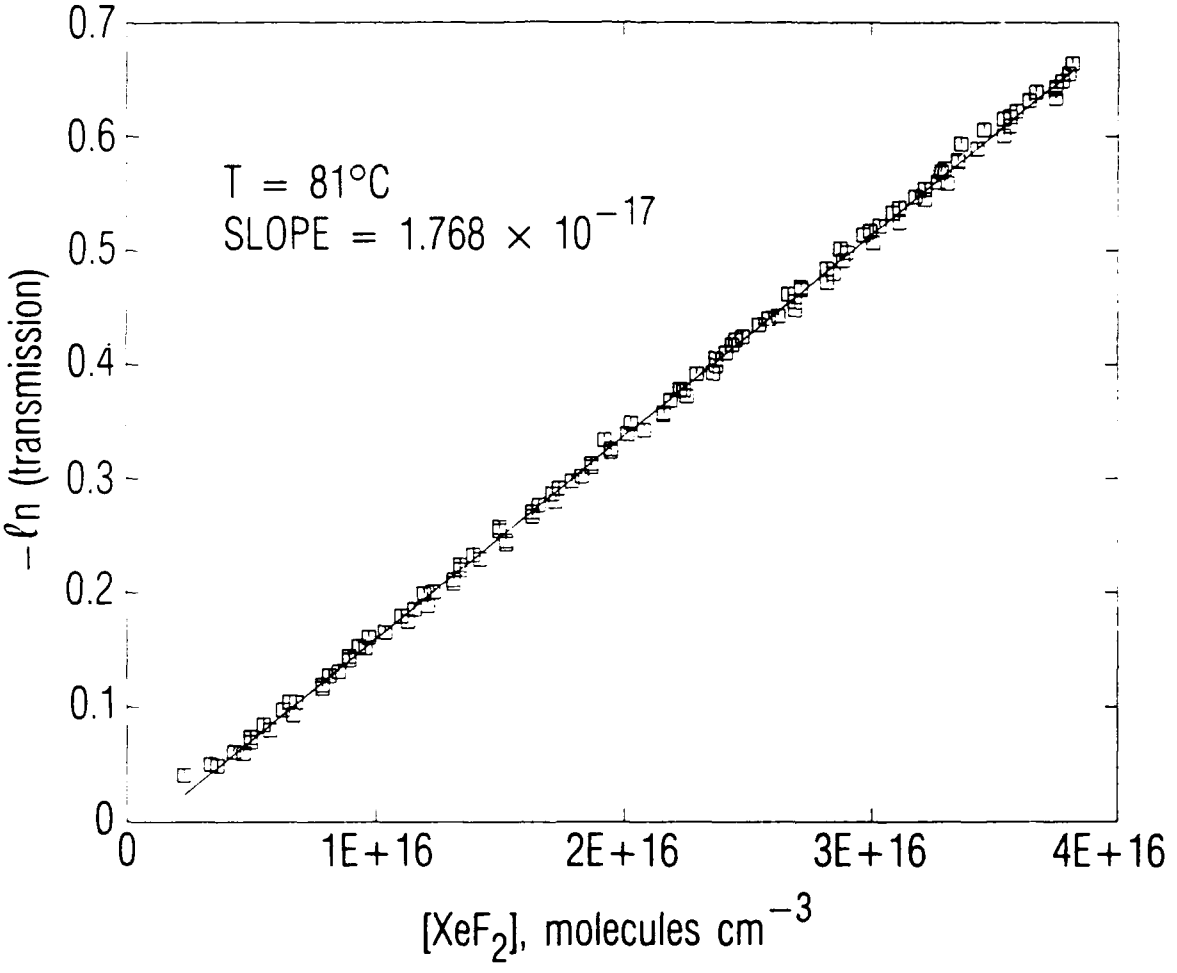

Fig. 4. Plot of XeF_2 absorption [-ℓn(transmission)] at 206 nm versus XeF_2 density.

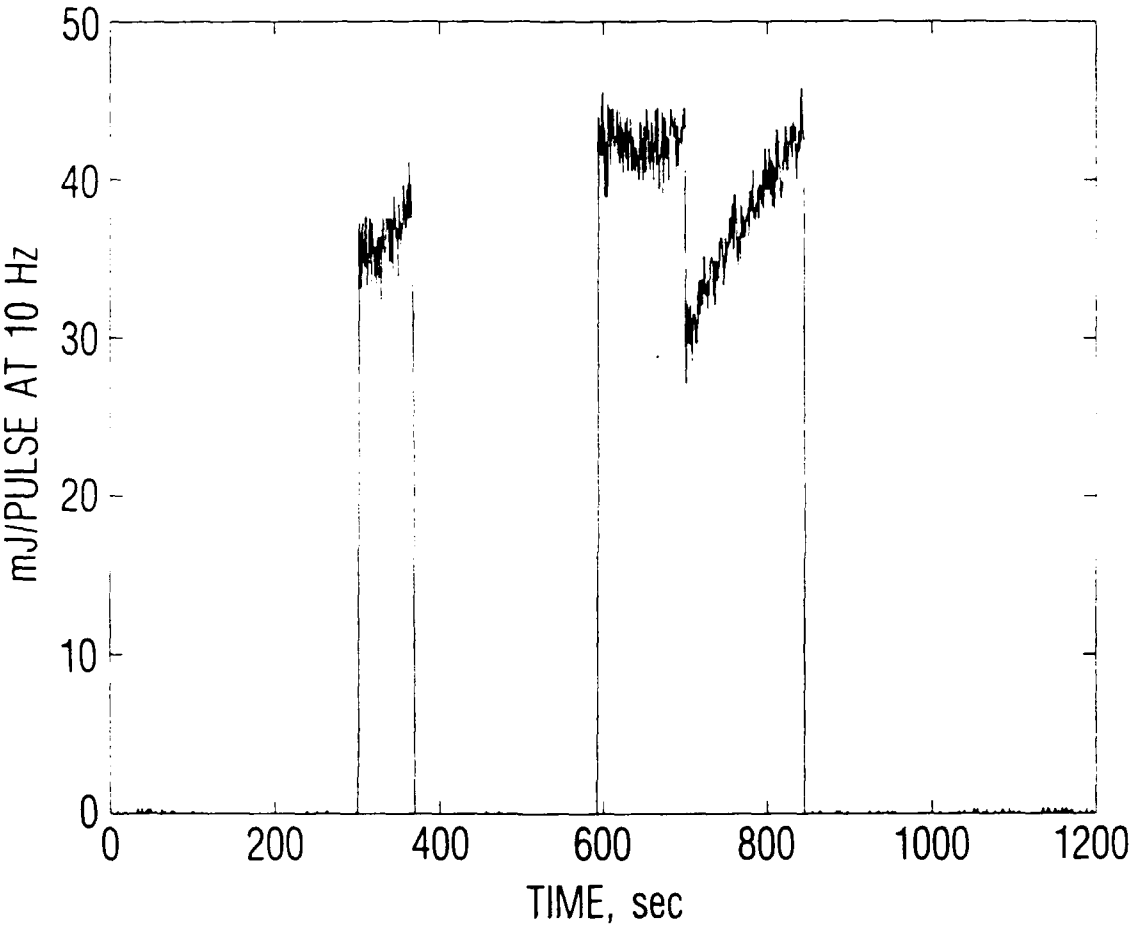

Fig. 5. Photolysis laser power measurement for quantum yield experiment.

recovery. The fraction of the laser pulse absorbed by the XeF_2 depends on the partial pressure of XeF_2 and its cross section at 193 nm. We have modeled this photolysis sequence using our measured cross section of 7.9×10^{-19} cm^2 and the assumption that the absorption of one photon results in the removal of one XeF_2 molecule, leading ultimately to the formation of one Xe and one F_2. The photolysis of XeF_2 can produce XeF in the B state as well as in the X state. However, radiative decay of the B state to the X state occurs in about 14 nsec.[8] The X state of XeF dissociates to Xe + F in a few microseconds.[16] The F atoms recombine on the walls to form F_2. The result of these processes is that two molecules are produced for each molecule dissociated, with an accompanying increase in pressure. Our calculated pressure profile for the laser sequence in Fig. 5 is shown in Fig. 6, along with the measured pressure history. The excellent agreement of the calculated and measured pressure histories justifies the assumption of the 100% yield of dissociated XeF_2 per photon absorbed.

B. OMA MEASUREMENTS OF XeF(B) EMISSION

We have recorded the B-state emission spectrum with an optical multichannel analyzer (OMA). The spectrum obtained from low-pressure photodissociation of XeF_2 at 21°C is shown in Fig. 7. The spectrum exhibits banded structure on top of an underlying continuum. The continuum may result from transitions from the B state to unbound states above the dissociation limit of the ground state. Figure 8 shows the spectrum with the continuum subtracted, leaving only the banded emission features. Integrations of the banded spectrum and the underlying continuum indicate that 10% of the B-state emission goes to the bound vibrational levels of the ground electronic state and 90% goes to unbound levels. Therefore, the quantum yield of bound states of XeF(X,v) via the B state is rather small.

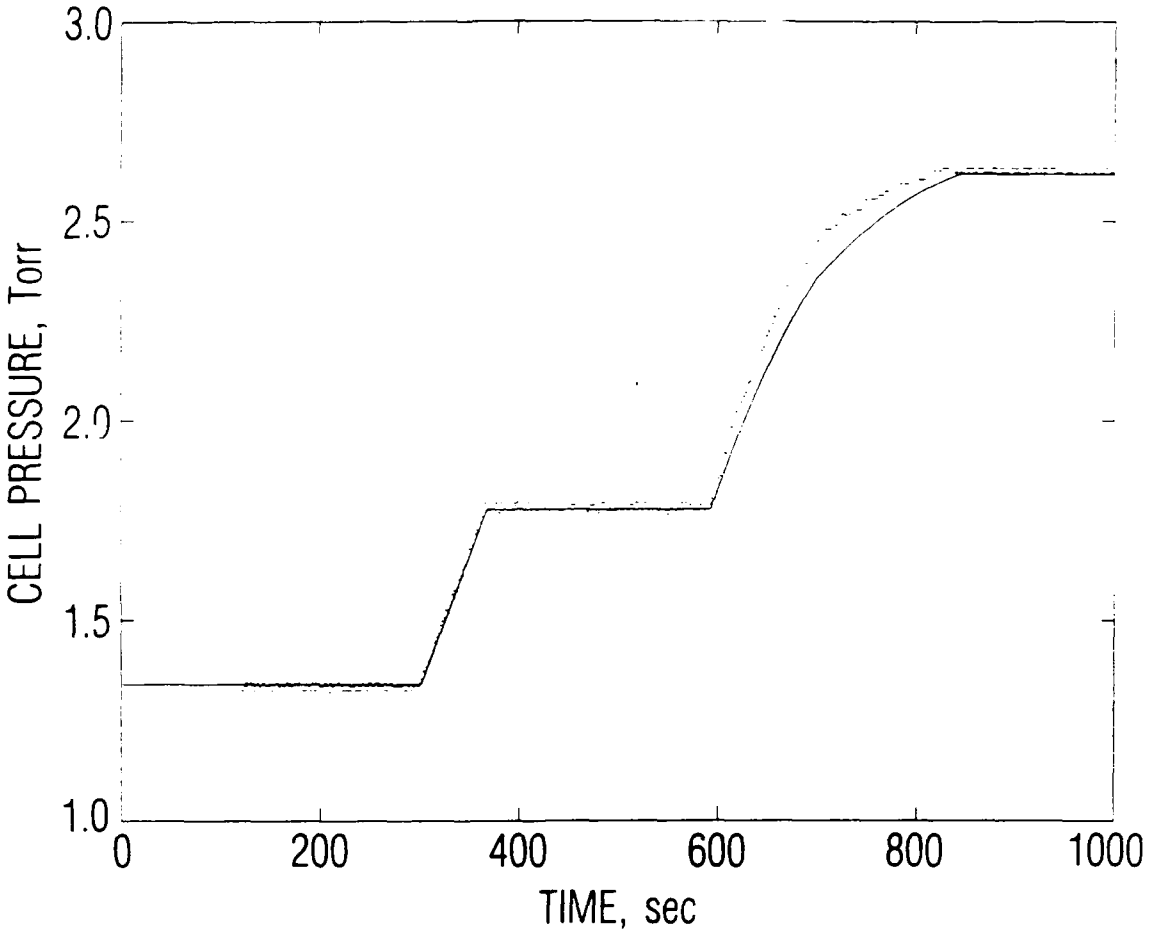

Fig. 6. Measured and calculated cell pressures versus time in quantum yield experiment.

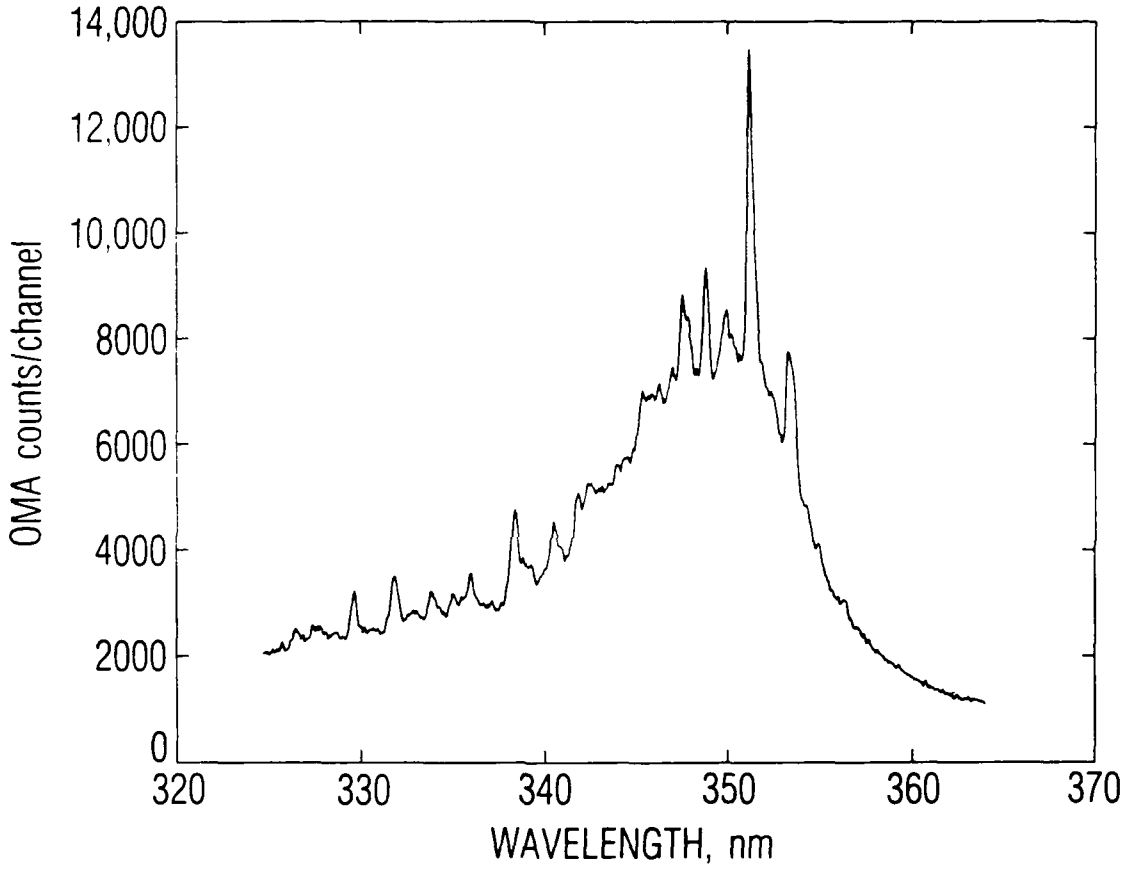

Fig. 7. XeF(B) emission spectrum from the photolysis of XeF_2 at 193 nm.

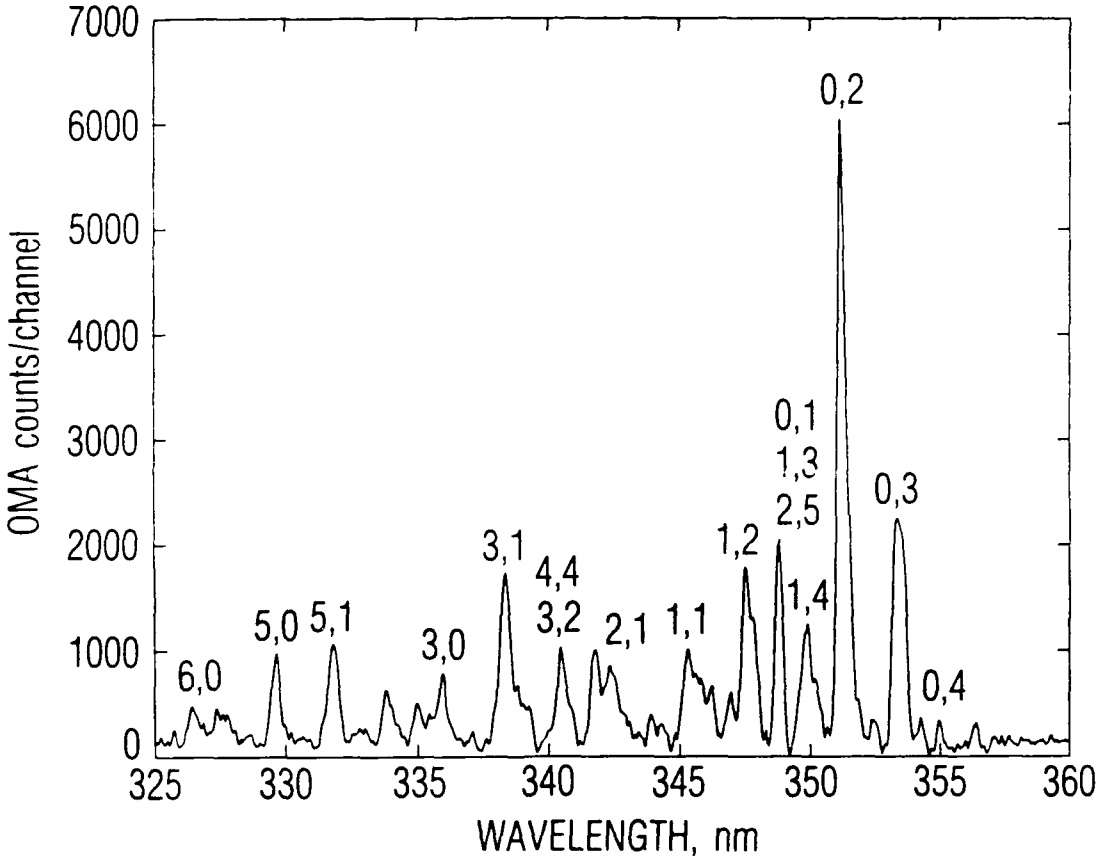

Fig. 8. The XeF(B) emission spectrum of Fig. 7 with the underlying continuum subtracted.

III. DISCUSSION AND SUMMARY

In Ref. 12, Black et al. plot absorption coefficients of XeF_2 that they and two other groups measured between 142 and 280 nm. Measurements between 142 and 210 nm by Black et al. overlap measurements reported by Jortner et al.[17] between 203 and 280 nm, but they disagree by a factor of 2.4 in the region of overlap. Our measurement of 0.0262 $(Torr\text{-}cm)^{-1}$ or 7.9×10^{-19} cm^2 at 193 nm is approximately 32% larger than the value of 6.0×10^{-19} cm^2 measured by Black et al. Likewise, our value of 2.56×10^{-19} cm^2 at 206 nm is 34% larger than their value of 1.87×10^{-19} cm^2. On the other hand, our value of 8.0×10^{-20} cm^2 at 253 nm is less than the value of 1.6×10^{-19} cm^2 reported by Jortner et al.[17] When both sets of data in Ref. 12 are scaled to agree with our three data points they agree in the region of overlap. This agreement appears to suggest that the difficulty of measuring the partial pressure of XeF_2 accounts for the systematic source of the discrepancy in the previously reported data. It should be noted that the absorption coefficients of Jortner et al. plotted in Ref. 12 were recalculated by Black et al. on the basis of the vapor pressure data of Schreiner et al.[18]

Our XeF_2 absorption coefficient measured at 206 nm had a value of 2.56×10^{-19} cm^2 at 21°C and a 16% larger value of 2.96×10^{-19} cm^2 at 81°C. This 16% increase with temperature may indicate the presence of hot band absorption by XeF_2; however, a more complete temperature study is required before conclusions can be drawn.

In the present studies we determined that the absorption of a 193-nm photon leads to the removal of one molecule of XeF_2. We cannot state, however, the fraction of XeF molecules produced in the B state or the X state. The energetic threshold[19] for the production of the B state is 204 nm. Therefore, a photon at 193 nm has sufficient energy to produce XeF(B) with 2790 cm^{-1} of vibrational/rotational energy, which corresponds to a vibrational level of about $v = 9$ in the B state. Black et al.[12] reported the B-state quantum yield for the photolysis of XeF_2 to be

0.9 (+0.1,-0.2) between 146 and 172 nm. They estimate, however, that the quantum yield of the B state at 193 nm is less than 1%.[20] Bibinov et al.[21] have also reported a quantum yield of about 0.8% at 193 nm. Although their quantum yield measurements are significantly lower than those of Black et al. in the important range of 142 to 175 nm, both groups report low quantum yields of the B-state for 193-nm photolysis.

We recorded, with an optical multichannel analyzer, the emission from the B state following the photolysis of XeF_2 at 193 nm. The OMA measurements indicate that only 10% of the B state radiates to the bound vibrational levels of the ground state, and the other 90% radiates to unbounded levels above the dissociation limit. Therefore, even if the dissociation products of Xe and F atoms are not produced directly by the XeF_2 photolysis, they are produced subsequently by the radiative decay of the B state to the unbound states, which dissociate rapidly.

In summary, the present measurements of the XeF_2 absorption at 193 and 253 nm appear to resolve the discrepancy in the absorption measurements plotted in Fig. 1 of Ref. 12. Adjusting the data in that figure to match our values at these two wavelengths brings the two sets of measured absorption coefficients into agreement in their overlapping wavelength interval. We determined experimentally that the absorption of one photon at 193 nm leads to the dissociation of one XeF_2 molecule.

REFERENCES

1. N. G. Basov, V. S. Zuev, A. V. Kanev, L. D. Mikheev, and D. B. Stavrovskii, Sov. J. Quantum Electron. 9, 629 (1979).

2. V. S. Zuev, L. D. Mikheev, and D. B. Stavrovskii, Sov. J. Quantum Electron. 14, 1174 (1984).

3. N. G. Basov, V. S. Zuev, D. B. Stavrovskii, and V. I. Yavlooi, Sov. J. Quantum Electron. 7, 1401 (1977).

4. D. J. Eckstrom and H. C. Walker, IEEE J. Quantum Electron. QE-18, 176 (1982).

5. G. N. Kashnikov, N. P. Kozlov, V. A. Reznikov, and V. A. Sorokin, Sov. J. Quantum Electron. 14, 1422 (1984).

6. V. S. Zuev, G. N. Kashnikov, N. P. Kozlov, V. A. Reznikov, V. K. Orlov, Yu. S. Protasov, and V. A. Sorokin, Sov. J. Quantum Electron. 16, 1665 (1986).

7. R. W. F. Gross, L. E. Schneider, S. T. Amimoto, "XeF Laser Pumped by High-Power Sliding Discharges," presented at the Third Int. Laser Science Conf., Atlantic City, NJ (1-5 November 1987).

8. J. G. Eden and R. W. Waynant, Opt. Lett. 2, 13 (1978).

9. J. G. Eden and R. W. Waynant, J. Chem. Phys. 68, 2850 (1978).

10. H. C. Brashears, D. W. Setser, and D. Desmartineau, Chem. Phys. Lett. 48, 84 (1977).

11. H. C. Brashears and D. W. Setser, J. Chem. Phys. 76, 4932 (1982).

12. G. Black, R. L. Sharpless, D. C. Lorents, D. L. Huestis, R. A. Gutcheck, T. D. Bonifield, D. A. Helms, and G. K. Walters, J. Chem. Phys. 75, 4840 (1981).

13. H. Helm, L. E. Jusinski, D. C. Lorents, and D. L. Huestis, J. Chem. Phys. 5, 1796 (1984).

14. S. F. Fulghum, M. S. Feld, and A. Javan, Appl. Phys. Lett. 35, 247 (1979).

15. S. F. Fulghum, M. S. Feld, and A. Javan, IEEE J. Quantum Electron. 16, 815 (1980).

16. J. F. Bott, R. F. Heidner, J. S. Holloway, J. B. Koffend, and M. A. Kwok, J. Chem. Phys. 89, 4154 (1988).

17. J. Jortner, E. G. Wilson, and S. A. Rice, Noble-Gas Compounds, ed. H. H. Hyman, University of Chicago, Chicago, IL (1963).

18. F. Schreiner, G. N. McDonald, C. L. Cherick, J. Phys. Chem. 72, 1162 (1968).

19. P. Tellinghuisen, J. Tellinghuisen, J. A. Coxon, J. E. Velazco, and D. W. Setser, J. Chem. Phys. 68, 5187 (1978).

20. G. Black and D. L. Huestis, personal communication to R. F. Heidner, February 1988.

21. N. K. Bibinov, I. P. Vinogradov, L. D. Mikheev, and D. B. Stavrovskii, Sov. J. Quantum Electron. 11, 1178 (1981).

LABORATORY OPERATIONS

The Aerospace Corporation functions as an "architect-engineer" for national security projects, specializing in advanced military space systems. Providing research support, the corporation's Laboratory Operations conducts experimental and theoretical investigations that focus on the application of scientific and technical advances to such systems. Vital to the success of these investigations is the technical staff's wide-ranging expertise and its ability to stay current with new developments. This expertise is enhanced by a research program aimed at dealing with the many problems associated with rapidly evolving space systems. Contributing their capabilities to the research effort are these individual laboratories:

Aerophysics Laboratory: Launch vehicle and reentry fluid mechanics, heat transfer and flight dynamics; chemical and electric propulsion, propellant chemistry, chemical dynamics, environmental chemistry, trace detection; spacecraft structural mechanics, contamination, thermal and structural control; high temperature thermomechanics, gas kinetics and radiation; cw and pulsed chemical and excimer laser development including chemical kinetics, spectroscopy, optical resonators, beam control, atmospheric propagation, laser effects and countermeasures.

Chemistry and Physics Laboratory: Atmospheric chemical reactions, atmospheric optics, light scattering, state-specific chemical reactions and radiative signatures of missile plumes, sensor out-of-field-of-view rejection, applied laser spectroscopy, laser chemistry, laser optoelectronics, solar cell physics, battery electrochemistry, space vacuum and radiation effects on materials, lubrication and surface phenomena, thermionic emission, photosensitive materials and detectors, atomic frequency standards, and environmental chemistry.

Computer Science Laboratory: Program verification, program translation, performance-sensitive system design, distributed architectures for spaceborne computers, fault-tolerant computer systems, artificial intelligence, microelectronics applications, communication protocols, and computer security.

Electronics Research Laboratory: Microelectronics, solid-state device physics, compound semiconductors, radiation hardening; electro-optics, quantum electronics, solid-state lasers, optical propagation and communications; microwave semiconductor devices, microwave/millimeter wave measurements, diagnostics and radiometry, microwave/millimeter wave thermionic devices; atomic time and frequency standards; antennas, rf systems, electromagnetic propagation phenomena, space communication systems.

Materials Sciences Laboratory: Development of new materials: metals, alloys, ceramics, polymers and their composites, and new forms of carbon; nondestructive evaluation, component failure analysis and reliability; fracture mechanics and stress corrosion; analysis and evaluation of materials at cryogenic and elevated temperatures as well as in space and enemy-induced environments.

Space Sciences Laboratory: Magnetospheric, auroral and cosmic ray physics, wave-particle interactions, magnetospheric plasma waves; atmospheric and ionospheric physics, density and composition of the upper atmosphere, remote sensing using atmospheric radiation; solar physics, infrared astronomy, infrared signature analysis; effects of solar activity, magnetic storms and nuclear explosions on the earth's atmosphere, ionosphere and magnetosphere; effects of electromagnetic and particulate radiations on space systems; space instrumentation.